Available online at www.sciencedirect.com
SCIENCE DIRECT®
ELSEVIER
Applied Surface Science 215 (2003) 169–177
applied surface science
www.elsevier.com/locate/apsusc

Electron spectroscopy of nanodiamond surface states

P.I. Belobrov[a,*], L.A. Bursill[b], K.I. Maslakov[c], A.P. Dementjev[c]

[a]*Molecular Architecture Group, Institute of Biophysics SB RAS and UNESCO chair of Krasnoyarsk State Technical University, Krasnoyarsk 660036, Russia*
[b]*School of Physics, The University of Melbourne, Parkville, Victoria 3010, Australia*
[c]*RRC Kurchatov Institute, Moscow 123182, Russia*

Received 12 August 2002; received in revised form 27 January 2003

Abstract

Electronic states of nanodiamond (ND) were investigated by PEELS, XPS and CKVV Auger spectra. Parallel electron energy loss spectra (PEELS) show that the electrons inside of ND particles are sp^3 hybridized but there is a surface layer containing distinct hybridized states. The CKVV Auger spectra imply that the HOMO of the ND surface has a shift of 2.5 eV from natural diamond levels of σ_p up to the Fermi level. Hydrogen (H) treatment of natural diamond surface produces a chemical state indistinguishable from that of ND surfaces using CKVV. The ND electronic structure forms $\sigma_s^1\sigma_p^2\pi^1$ surface states without overlapping of π-levels. Surface electronic states, including surface plasmons, as well as phonon-related electronic states of the ND surface are also interesting and may also be important for field emission mechanisms from the nanostructured diamond surface.

Keywords: Nanodiamond; Surface states; PEELS; XPS; Auger electron spectroscopy

1. Introduction

The surface states on reconstructed diamond (1 1 1), the atomic and electronic structure of diamond surface, and the effect of hydrogen on the surface electrical conductivity of diamond (1 1 0) have been extensively studied [1–3]. The fact that Auger decay in diamond (1 1 0) surfaces after hydrogen treatment is similar to that of nanodiamond (ND) [4] has lead to the present research.

For practical applications, solid porous semiconductor material made from ND [5] has a special place among low-dimensional semiconductors [6] and hydrogen treatment of diamond is important for effective field emission from nanostructured diamond [7]. Changing the mass ratio of sp^2/sp^3 phases from 0 up to 50% increases the electronic conductance of nanodiamond/pyrocarbon composite (NDC) material by 12 orders of magnitude [8] and has a strong influence on the field emission properties of NDC [9].

Nuclear magnetic resonance (NMR) and electron paramagnetic resonance (EPR) results for nanodiamond spheres and polyhedra of diameter 3–6 nm imply a concentration of unpaired spins of 4×10^{19} spins/g (i.e. $\sim$1 spin per ND cluster). The g-factor $= 2.0027 \pm 10^{-4}$ and the width of the EPR line $\Delta H = 0.86 \pm 0.02$ mT are not sensitive to the constitution and nature of functional surface groups, nor on the temperature, composition, or fabrication and purification methods of ND. The NMR method using ^{13}C showed that ND contains 30% normal sp^3 bonds and 70% chemically-distinct sp^3 bonds with overall a total

* Corresponding author. Tel.: +7-3912-495-590; fax: +7-3912-433-400.
E-mail address: pit@ktk.ru (P.I. Belobrov).

0169-4332/03/$ – see front matter
doi:10.1016/S0169-4332(03)00287-3

of only one unpaired electron per ND [10]. The invariance of paramagnetic properties for ND over a temperature range of 5–300 K has been confirmed independently by Shames et al. [11].

Recent electron, CKVV (the core hole is in the carbon K level and both final-state holes are in valence levels) Auger, EPR and NMR spectroscopic and field emission property measurements of ND made by explosive synthesis are discussed below in terms of the low-dimensional surface states of nanocrystalline diamond.

2. PEELS and STEM of nanodiamond

Parallel electron energy loss spectroscopy (PEELS) data were recorded using a scanning transmission elec-

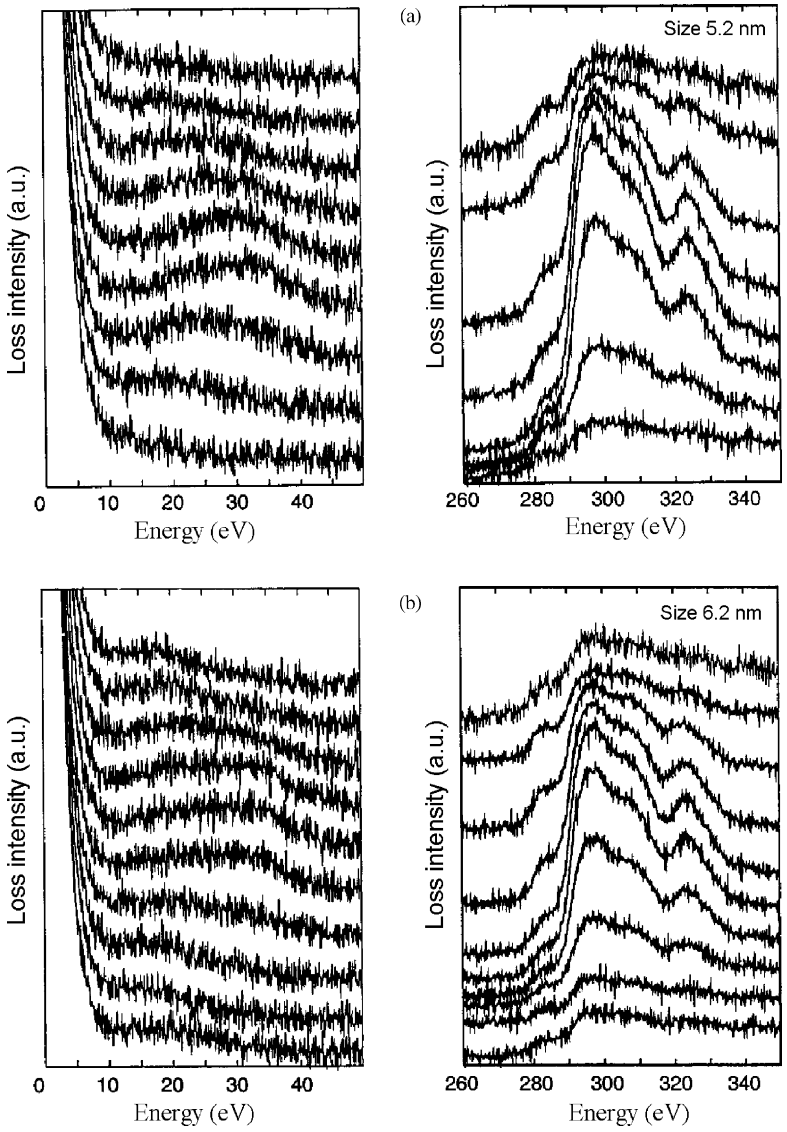

Fig. 1. Line scan parallel electron energy loss spectrum for low-loss (left) and core-loss (right) energy ranges for three ND particles of diameter (a) 5.2, (b) 6.2 and (c) 7.6 nm. At the low-loss range surface (12–24 eV) and bulk (30–33 eV) plasmons depend on a size of ND (see more in [13,14]). Pre-peak (280–295 eV) characterises ND at the core-loss range (see Section 2).

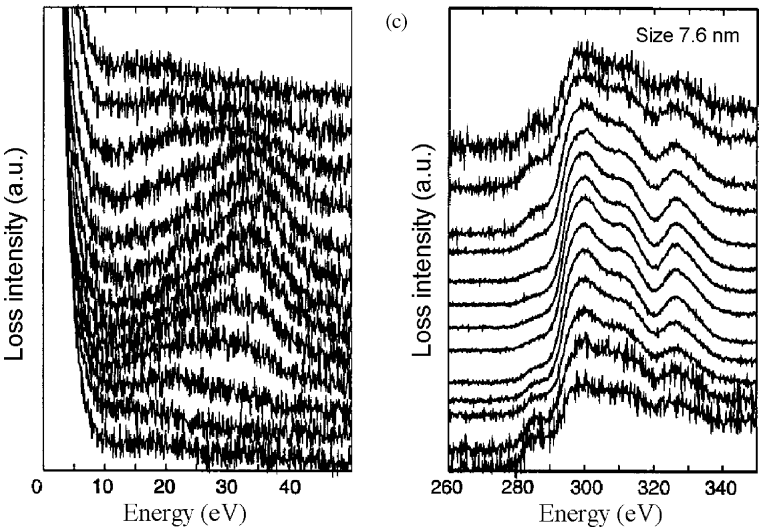

Fig. 1. (*Continued*).

tron microscope (STEM) at the Electron Microscope Unit, University of Sydney. A GATAN electron spectrometer (Model 666) was attached to a VG-HB601 STEM. PEELS data were obtained at 100 keV, the resolution of the spectrometer was estimated by measuring the full-width at half-maximum (FWHM) of the zero-loss peak; this was typically 0.5 eV. In this case the beam diameter was typically 1 nm, the objective aperture $D = 50$ μm and the objective convergence angle α was 13.7 mrad.

A 0.5 nm electron probe was scanned across single ND particles at step intervals of approximately 0.5 nm, and energy-loss spectra recorded at each step. Note that STEM and PEELS analysis requires a dose as high as 10^8 electrons per nm^2. STEM images recorded pre-scan and post-scan were used to assess specimen drift, specimen contamination and electron beam damage during data collection: results selected for analysis corresponded to no-drift, no contamination and no damage. Typically, ND was electron bombarded only for 2–4 min.

Detailed comparisons of the PEELS results for three particles, of apparent diameters 5–7 nm respectively are shown as Fig. 1(a)–(c) (see also discussion in [12]). Note that the intensities of the pre-peaks (280–295 eV) relative to the 300 eV diamond core-loss peaks are dependent on the size of the particle, decreasing as the size increases. The relative intensity of the pre-edge peak to the 300 eV peak also varies as the beam moves towards, through and away from the center of the particles. Notice also the symmetrical nature of the variation of the relative intensity of the pre-peak to the 300 eV core-loss peaks as the electron probe enters, crosses and then exits the spherical particle; with intensity maximum at the entrance surface, decreasing to a minimum at the center of the particle and then increasing back to the maximum value at the exit surface.

In order to attempt to make quantitative measurements of the above two effects we define the intensity of the pre-peak I_{pre} as:

$$I_{pre} = \frac{I_s}{(I_s + I_b)}$$

where I_s is the integrated intensity over the range 280–295 eV of the pre-edge spectrum of diamond. This is characteristic of the non-sp^3-bonded environment of the atoms under the electron probe, as it passes across the ND particle, I_b the integrated K core-loss intensity corresponding to the bulk of the diamond particle, over the range 295–340 eV; which is again dependent on the beam position on the ND particle. Detailed measurements and analyses [12] confirmed that the evolution of the relative intensity of the pre-peak to the 300 eV core-loss peak across the ND was indeed consistent with the proposition that the pre-peak (energy-loss near-edge fine structure, or ELNES) intensity was essentially due to modified or non-sp^3

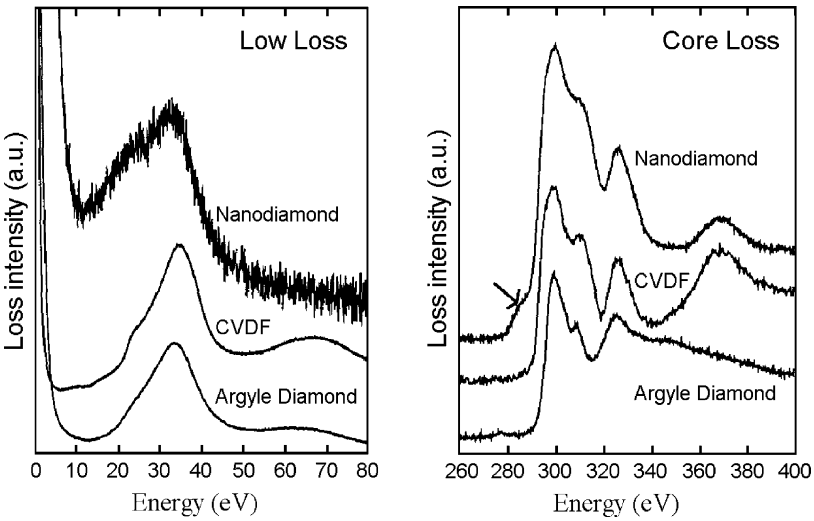

Fig. 2. Integral intensity of electron energy loss spectrum (left) low-loss and (right) core-loss ND diameter 7.6 nm, CVDF micron size diamond, and natural Argyle diamond using 100 keV electrons. Arrow labels pre-peak (see Section 2).

bonded surface states of carbon atoms and also that the pre-peak evolution effectively represents the variation of the ratio of surface to volume states intersecting the electron probe as it scans across the ND particles.

The integrated intensity (I) over the entire 7.6 nm diameter ND is compared with the reference PEELS data for CVD diamond and a gem-quality Argyle natural gem quality diamond are included for comparison in Fig. 2 (see detailed discussion in [12]).

These results emphasize the quite distinctive pre-edge phenomena observed for ND particles, compared to CVDF and gem quality diamond crystals. It is concluded that parallel electron energy loss spectroscopy shows that all electrons inside of ND particles are sp^3 hybridized, whereas altered sp^2/sp^3 states exist in a thin surface layer.

Evolution of the surface and bulk plasmon-loss peaks is also shown in Figs. 1(a)–(c) and 2; these are collective oscillations of the valence electrons and have been analyzed in considerable detail in [13–15].

3. CKVV Auger spectroscopy of nanodiamond

XPS and X-ray excited Auger electron spectra (XAES) were obtained using a VG Scientific ESCALAB MK II spectrometer. Photoelectron and Auger processes were excited by the un-monochromatized Al Kα X-ray source (1486.6 eV, resolution 1 eV). Use of a photon rather than an electron source for excitation of Auger emission enables calibration of spectra using the C 1s XPS peak and reduces sample damage.

The ND was deposited on a Si plate (10 mm × 15 mm) from an alcohol suspension in an ultrasonic bath. The surfaces of ND were analyzed in-situ before and after H-treatment. The H-treatment was carried out in the preparation chamber used a hot-filament (2300 K) and a partial pressure of H_2 of 10^{-6} mbar. The spiral W hot-filament was located 1 cm above the sample. The substrate temperature was about 700 K. The W filament temperature was measured using a pyrometer. All spectra were calibrated relative to the reference C 1s XPS peak (284.8 eV). The position of C 1s was determined with respect to the Ar $2p_{3/2}$ XPS peak at 241.3 eV after implantation of a small dose of Ar into ND. For comparison we used 3–6 nm ND of different producers (Krasnoyarsk, Snezhinsk and others).

Identification of the electronic states of carbon atoms on a ND surface is because the disperse state does not allow ultraviolet photoelectron spectroscopy (UPS) [16] to be applied. Therefore, Auger electron spectroscopy of the diamond surface (1 1 0) after H-treatment and the ND surface were carried out. They were found to be identical [4]. Thus, since a CKVV Auger spectrum is the self-convolution of the

density of states (DOS) [17,18], it is possible to suggest that the electronic state in the upper 2–3 atomic layers of ND are not very different to that for a crystalline diamond surface after H-treatment.

Pate showed [2] that the state of a diamond surface after H-treatment is characterized by a peculiarity in the photoelectron spectrum near the Fermi edge (E_F) with features similar to the π-bands of graphite. A comparable state was observed by Himpsel et al. [1]. The angle-integrated data was very similar to the behavior of the π-bands of graphite. However, the angle resolved data show that the surface state has not the same momentum distribution as the π-bands of graphite. Therefore the electronic state of the diamond surface after H-treatment must be characterized very carefully. It is useful to compare the Auger spectra of ND with the Auger spectrum of carbon atoms with different hybridization.

The comparison in Fig. 3 demonstrates agreement of the right-hand side gradients of the ND spectrum with that of polyethylene and its difference from graphite. But the various energy peaks of the spectrum do not allow identification of the chemical state in ND to sp^3.

Comparison of nanodiamond and high oriented pyrolytic graphite (HOPG) spectra with the self-convolution of the DOS taken from Murday et al. [17] is represented in Fig. 4. It can be seen that in ND case the $\pi \times \pi$ and $\sigma_s \times \sigma_p$ transitions are not realized. To date interpretation of CKVV Auger spectra have been problematic. In the contribution described in this paper qualitative evaluation allowed useful results to obtained. There are a $\sigma_p \times \pi$ contribution to the spectra and consequently π-bonds on surface, but they do not coincide with that in pure graphite. A state similar to Himpsel [1] and Pate [2] is observed. It is thought that the π-like bonds on surface structure correspond to the buckling or dimerized-chain models of Pandey [19]. Note that most of the surface bonds of this reconstruction are sp^3 with lines of dimers of a π-like bond. Recent ab-initio calculations of the atomic and electronic structure of clean and hydrogenated diamond (1 1 0) surfaces [20] confirmed the suggestion about π-like dimerization of ND surface.

From the Auger decay on the right hand side of the Auger spectra (Figs. 3 and 4) for polyethylene and ND it is possible to introduce by the following schemes. For polyethylene:

$$\mathrm{C}\,1s^2\sigma_s^1\sigma_p^3 + h\nu\,(\text{X-ray external}) \rightarrow \mathrm{C}\,1s^1\sigma_s^1\sigma_p^3 + \mathrm{e}$$

$$\mathrm{C}\,1s^1\sigma_s^1\sigma_p^3 \rightarrow \mathrm{C}\,1s^2\sigma_s^1\sigma_p^2 + h\nu\,(\text{X-ray inner})$$

$$\mathrm{C}\,1s^2\sigma_s^1\sigma_p^2 + h\nu\,(\text{X-ray inner}) \rightarrow \mathrm{C}\,1s^2\sigma_s^1\sigma_p^1 + \mathrm{e}\,(\text{Auger electron})$$

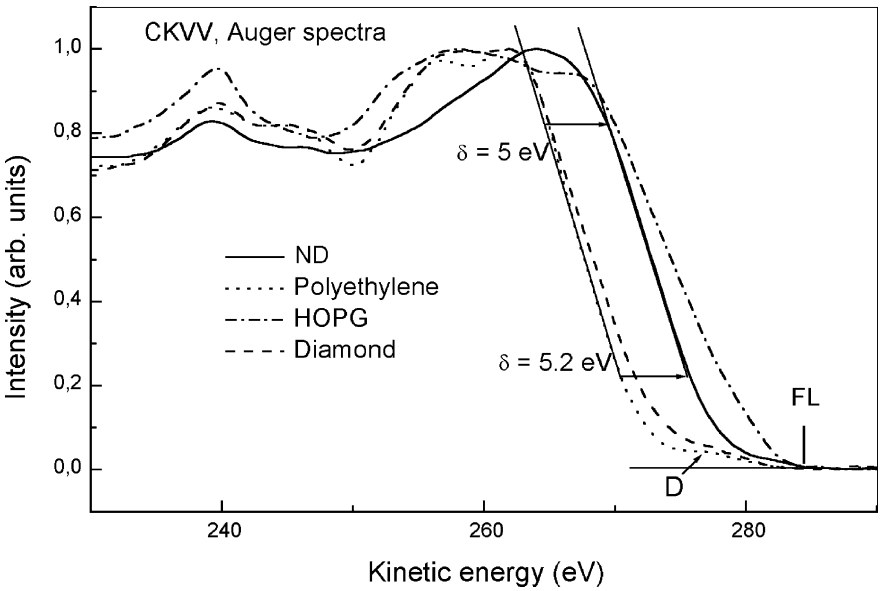

Fig. 3. CKVV Auger ND, HOPG, diamond and polyethylene. Region D is described in the text.

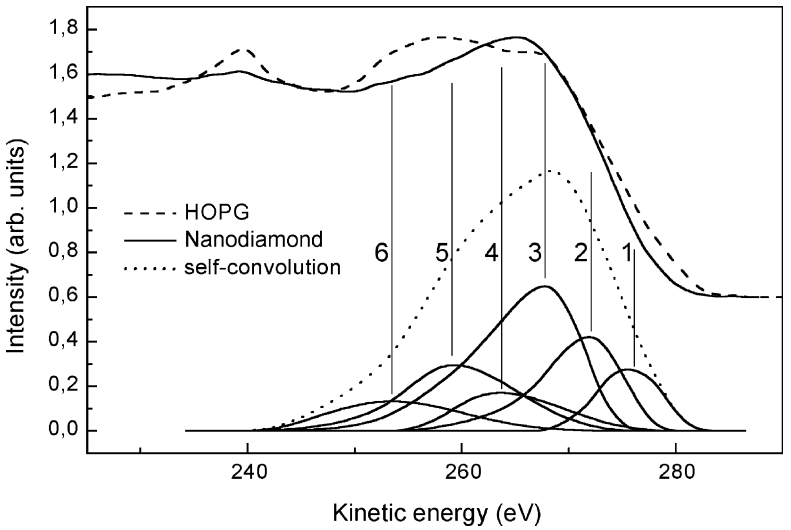

Fig. 4. CKVV Auger spectra from HOPG and nanodiamond with the self-convolution. $1-\pi\times\pi$; $2-\sigma_p\times\pi$; $3-\sigma_p\times\sigma_p$; $4-\pi\times\sigma_s$; $5-\sigma_p\times\sigma_s$; $6-\sigma_s\times\sigma_s$.

It is possible to suggest the following Auger decay schemes for ND:

$$\mathrm{C\,1s^2}\sigma_s^1\sigma_p^2\pi^1 + h\nu\,(\text{X-ray external}) \rightarrow \mathrm{C\,1s^1}\sigma_s^1\sigma_p^2\pi^1 + \mathrm{e}$$

$$\mathrm{C\,1s^1}\sigma_s^1\sigma_p^2\pi^1 \rightarrow \mathrm{C\,1s^2}\sigma_s^1\sigma_p^2\pi^0 + h\nu\,(\text{X-ray inner})$$

$$\mathrm{C\,1s^2}\sigma_s^1\sigma_p^2\pi^0 + h\nu\,(\text{X-ray inner}) \rightarrow \mathrm{C\,1s^2}\sigma_s^1\sigma_p^1\pi^0 + \mathrm{e}\,(\text{Auger electron})$$

These schemes allow understanding the similar declinations of the right hand side of spectrums for polyethylene and nanodiamond. The comparison demonstrates the validity of the suggestion of an opportunity of ND electronic structure to form $\sigma_s^1\sigma_p^2\pi^1$ surface states. Graphite has same $\sigma_s^1\sigma_p^2\pi^1$ surface states but π^0-hole is delocalized with large length of overlapping and consequently $\pi\times\pi$ convolution takes place in HOPG owing to π-band. This fact allows to suggest that ND π-levels are not overlapped since the curvature of ND surface prevents from formation a plane of symmetry and consequently the p_z orbitals do not form common π-band. Thus π^0-hole is localized in ND without overlapping of π-levels, i.e. p_z orbitals of nearest carbon atom overlap only, and that is opposed to graphite.

On the right hand side of Fig. 3 there is a visible spectral difference between diamond and polyethylene. It is explained by presence nanocarbon with sp^2 bonds on diamond surface. The multiple Auger-spectroscopy of natural diamond after a mechanical abrasion has not given consistent results. Note that an Auger spectrum of diamond after H-treatment is similar to the Auger spectra of ND [4]. In the case of polyethylene the spectra always were identical. Therefore, the Auger spectrum of polyethylene was used as the standard for sp^3 bonds.

The structure D (shown in Fig. 3) was observed in Auger spectra with sp^3 bonds not only when polyethylene was measured but also for other polymeric compounds with sp^3-bonds [21]. This part of a spectrum cannot be described by involvement of valence electrons. Ramaker [22] has offered interpretation of such state by resonant excitation of C 1s electron into an empty state (ES) and participation of the electrons in Auger decay:

$$\mathrm{C\,1s^2\,(VB)\,(ES)^0 + e \rightarrow C\,1s^1\,(VB)\,(ES)^1 + e}$$

$$\mathrm{C\,1s^1\,(VB)\,(ES)^1 \rightarrow C\,1s^2\,(VB)^{-1}\,(ES)^0}$$

The structure D (Fig. 3) was observed in the experiment by X-ray excitation of Auger holes. The energy distribution of secondary electrons is wide enough that there

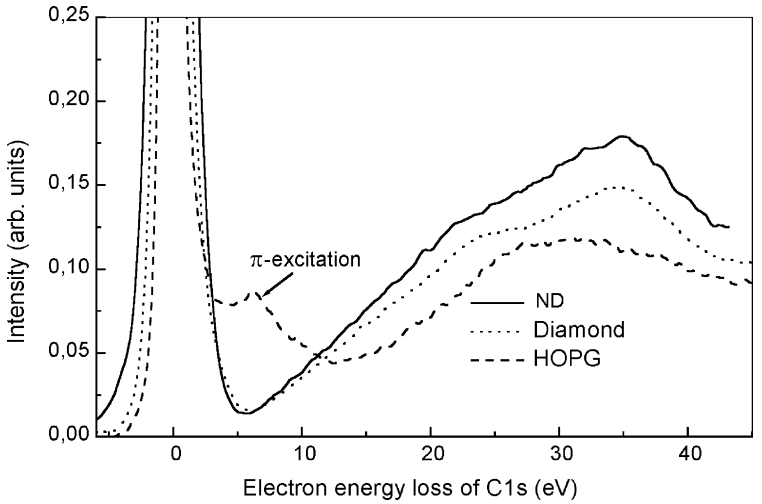

Fig. 5. Comparison of C 1s electron energy-loss spectrum of nanodiamond, diamond and graphite using X-ray excitation 1486.6 eV—Al Kα (see Section 3).

can be electrons capable of being located in a hypothetical hole. The Auger decay would be following:

$$\mathrm{C\,1s^2\,(VB)}\,T^0 + \text{X-ray} \rightarrow \mathrm{C\,1s^1\,(VB)}\,T^0 + \text{e-primary} + \text{e-secondary}$$

$$\mathrm{C\,1s^1\,(VB)}\,T^0 + \text{e-secondary} \rightarrow \mathrm{C\,1s^1\,(VB)}\,T^1$$

$$\mathrm{C\,1s^1\,(VB)}\,T^1 \rightarrow \mathrm{C\,1s^2\,(VB)^{-1}}\,T^0 + \mathrm{e\,(Auger)}$$

where T is some located level in a forbidden region. At the moment it is not possible to tell if it is localized before ionization of C $1s^2$ or its localization and the occupation takes place after ionization of C $1s^2$.

Electron energy loss of C 1s photoelectrons is also interesting for a characterization of ND. Fig. 5 shows the energy loss spectra of ND, diamond and graphite. The ND spectrum has no features of graphite. As the information depth of Auger electrons ($E_K = 270$ eV) and C 1s photoelectrons ($E_K = 1200$ eV) differ by so much, there are no contradictions with Auger data that demonstrate π-states. According to [23] these electrons have an information depth of 2 and 7 monolayers respectively. Therefore in a ND spectrum the π-excitation is not observed. The energy loss spectrum of ND is close to a spectrum of diamond.

H-treatment of a natural diamond surface produces the same chemical state to that on ND surfaces, i.e. ND-like chemical states are important for field emission from surface states of nanostructured diamond.

4. Calculation of model molecules

The well-known 2 × 1 reconstruction for the (1 0 0) face is observed for the diamond cluster [24]. Metastable reconstructions of the diamond (1 1 1) surface were explained by interplay between diamond and graphite-like bonding [25]. Large-scale calculation of optical dielectric functions of diamond nanocrystallites [26] and tight binding modelling of properties related to field emission from nanodiamond clusters [27] have been made recently.

Described above electron, CKVV Auger, EPR and NMR spectroscopic and field emission property measurements of ND are needed for the discussion in terms of delocalized electronic wave developed in the theory [29,30], taking into account clear qualitative physical picture and the theoretical predictions of one- and two-dimensional surface states [31]. Until now, however, there is no self-consistent model of electronic-vibration surface states.

Here the main changes of band structure for saturated, radical and complete dehydrated states using simple molecular models (see Fig. 6a–c) are illustrated. Calculations of spherically symmetric homologues in the series adamantane ($C_{10}H_{16}$), pentamantane ($C_{22}H_{28}$), $C_{60}H_{60}$, and $C_{66}H_{64}$ have established changes in electronic structure independent of the homologue number. On formation of a radical state the discrete molecular levels are eliminated which lie

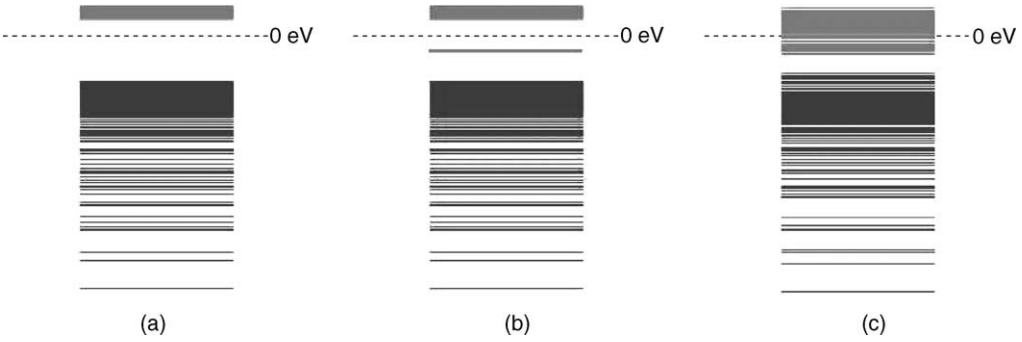

Fig. 6. Band diagrams (HOMO and LOMO) of: (a) $C_{60}H_{60}$ $E_g = 12.5$ eV; (b) radical state $C_{60}H_{60} \rightarrow C_{60}H_{59}^{\bullet}$; (c) complete dehydrated state $C_{60}H_{60} \rightarrow C_{60}$ (relaxed) $E_g = 5.3$ eV.

between HOMO and LUMO levels; resulting in the Tamm level (band) of the unpaired electron (hole-state) lying approximately at the forbidden gap of nanodiamond. Note that Tamm surface electronic states are expected due to electrons confined to surface edges and faces respectively (vicinal facets for spheres and simply facets for polyhedra). Therefore, to explain the basic properties of ND it is necessary to recognize the formation of a stable radical state, which effectively neutralizes the surface charge [10,28] with a necessary reconstruction of the interface between the diamond core or skeleton and the surface terminating functional groups, particularly hydrogen (H) at the surface. Depending on the ambient gas and temperature there are dynamic electron/phonon (Tamm–Lifshitz–Pekar) states and surely electron–phonon coupling (exciton and polaron type states involving the surface atoms and electronic ⟨hole⟩ states are still under investigation) associated with this interface. These properties define the main features of diamond molecule and are consistent with the semiconductor performance of nanodiamond. The theoretical analysis of surface electronic states of NDC requires more work to demonstrate existence of one-dimensional band of surface states and cooperative behavior of Tamm electrons in ND.

5. Discussion

The fact that a 3.0 (4.0) nm diameter ND contains 73 (57)% of its bonds within a spherical shell of depth 0.25 nm, at the surface (see Table 3 of [15]), together with the NMR result that ND contains 70% chemically distinct sp^3 bonds, implies that the latter can be identified as the surface states. Thus each ND macromolecule consists of a three-dimensional diamond core containing normal paired electron states and an effectively two-dimensional surface layer containing modified sp^3 bonds at or near the surface plus approximately one net unpaired electron per ND.

Since there is a very strong tendency for the surface bonding electrons to pair; then the net number of unpaired electrons must be either 1 or 0; note that some ND particles may exist with 0 unpaired electrons. The result that only one unpaired electron per ND cluster is seen by paramagnetic experiments may be a statistical result, rather than a fundamental characteristic of ND. In fact it is more correct to say the majority of the carbon bonds at the surface (approximately 350 carbons per ND of diameter 3 nm) are indeed saturated; either by surface relaxation by a Pandey-type mechanism, in the case of clean carbon surfaces, or by termination with H atoms in the case of hydrogenated nanodiamonds [19,20].

The surface of a nanodiamond is an inert state to an ambient medium due to all of the possible surface depolarization mechanisms. A surface of nanodiamond and CVD diamond after hydrogen treatment have sp^3 hybridization but the Tamm surface electrons have displaced σ_p level to a Fermi level of 2.5 eV compared with a standing σ_p in diamond. The upper occupied levels lie near the Fermi level. Practically this is the physical basis of surface conductivity. Note that p-type surface conductivity with a hole density approximately 10^{13} per cm^2 is typical for CVD and ND [3,8].

6. Conclusion

The H-treatment of natural diamond surface produces the same chemical state that was observed for of ND surfaces. The ND electronic structure forms the $\sigma_s^1\sigma_p^2\pi^1$ surface states without overlapping of π-levels.

ND-like chemical states are important for field emission mechanism from surface states of nanostructured diamond. For example, comparative analysis of electronic, semiconductor and field emission properties of NDC and other low-dimensional materials from ND may support the conjecture that pre-breakdown charging and discharging processes having fractal panicles are necessary for field emission of electrons from carbon materials.

Acknowledgements

The work was supported in part by Farmsum Associates and Printable Field Emitters Ltd. Many thanks A.Y. Khazov, M.J. Kelly, R.G. Forbes, S.R.P. Silva, and W. Taylor for productive discussions on field emission from low dimensional surface states.

References

[1] F.J. Himpsel, D.E. Eastman, P. Heimann, J.F. Van der Veen, Phys. Rev. B 24 (1981) 7270.
[2] B.B. Pate, Surf. Sci. 165 (1986) 83.
[3] B.L. Mackey, J.N. Russell Jr., P.E. Pehrsson, J.E. Crowell, J.E. Butler, Diamond Mater. IV (1995) 455.
[4] A.P. Dementjev, K.I. Maslakov, O.O. Zabusov, New Diamond Frontier Carbon Technol. 12 (2002) 11.
[5] S.K. Gordeev, S.G. Zhukov, Y.I. Nikitin, V.G. Poltoratskii, Inorg. Mater. 31 (1995) 434.
[6] M.J. Kelly, Low-Dimensional Semiconductors, Clarendon Press, Oxford, 1995, p. 546.
[7] W. Zhu, G.P. Kochanski, S. Jin, Science 282 (1998) 1471.
[8] S.K. Gordeev, P.I. Belobrov, N.I. Kiselev, E.A. Petrakovskaya, T.C. Ekstrom, in: Proceedings of the Material Research Society Symposium on Microcrystalline and Nanocrystalline Semiconductors, vol. 638, 2001, pp. F18.4.1–F18.4.16.
[9] A.V. Karabutov, V.D. Frolov, V.I. Konov, V.G. Ralchenko, S.K. Gordeev, P.I. Belobrov, J. Vac. Sci. Technol. B 19 (2001) 965.
[10] P.I. Belobrov, S.K. Gordeev, E.A. Petrakovskaya, O.V. Falaleev, Doklady Phys. 46 (2001) 965.
[11] A.I. Shames, A.M. Panich, W. Kempiński, A.E. Alexenskii, M.V. Baidakova, A.T. Dideikin, V.Yu. Osipov, V.I. Siklitski, E. Osawa, M. Ozawa, A.Ya. Vul', J. Phys. Chem. Solids 63 (2002) 1993.
[12] J.L. Peng, S. Bulcock, P.I. Belobrov, L.A. Bursill, Int. J. Modern Phys. B 15 (2001) 4071.
[13] R.P. Fehlhaber, L.A. Bursill, Phys. Rev. B 60 (1999) 14147.
[14] J.L. Peng, R.P. Fehlhaber, L.A. Bursill, D.G. McCulloch, J. Appl. Phys. 89 (2001) 6204.
[15] L.A. Bursill, A.L. Fullerton, L.N. Bourgeois, Inter J. Mod. Phys. B 15 (2001) 4087.
[16] E. Maillard-Schaller, O.M. Kuettel, L. Diederich, L. Schlapbach, V.V. Zhirnov, P.I. Belobrov, Diam. Rel. Mater. 8 (1999) 805.
[17] J.S. Murday, B.I. Dunlap, F.L. Hutson, P. Oelhafen, Phys. Rev. B 24 (1981) 4764.
[18] J.E. Houston, J.W. Rogers Jr., R.R. Rye, F.L. Hutson, D.E. Ramaker, Phys. Rev. B 34 (1986) 1215.
[19] K.C. Pandey, Phys. Rev. B 25 (1982) 4338.
[20] G. Kern, J. Hafner, Phys. Rev. B 56 (1997) 4203.
[21] G. Beamson, D. Briggs, High Resolution XPS of Organic Polymers: The Scienta ESCA 300 Database, Wiley, England, 1992, pp. 182–224.
[22] D.E. Ramaker, J. Vac. Sci. Technol. A 7 (1989) 1614.
[23] C. J. Powell, A. Jablonski, NIST Electron Inelastic-Mean-Free-Path Database- Version 1.1, National Institute of Standards and Technology, Gaithersburg, MD, 2000.
[24] M. Menon, K.R. Subbaswamy, M. Sawtarie, Phys. Rev. B 48 (1993) 8398.
[25] A.V. Petukhov, D. Passerone, F. Ercolessi, E. Tosatti, A. Fasolino, Phys. Rev. B 61 (2000) R10590.
[26] Y. Kurokawa, S. Nomura, T. Takemori, Y. Aoyagi, Phys. Rev. B 61 (2000) 12616.
[27] D.A. Areshkin, O.A. Shenderova, V.V. Zhirnov, A.F. Pal, J.J. Hren, D.W. Brenner, Mat. Res. Soc. Proc. 621 (2000) R.5.161.
[28] I.E. Tamm, Z. Phys. Sowjetunion 1 (1932) 733.
[29] R.H. Fowler, Proc. Roy. Soc. A141 (1933) 56.
[30] E.T. Goodwin, Proc. Camb. Phil. Soc. 35 (1939) I-205, II-221, III-232.
[31] I.M. Lifshitz, S.P. Pekar, Usp. Fiz. Nauk 56 (1955) 531.